Original Research Article

EVALUATION OF ACTIVATED CARBON FROM RAPHIA PALM NUT ENDOCARP AS ADSORBENT FOR SOLID ADSORPTION REFRIGERATION

Abstract: Activated carbon was produced from powdered Raphia palm nut endocarp (REAC) using H_3PO_4 and $CaCl_2$ as activators before carbonization, and the responses studied to investigate its suitability for solid adsorption refrigeration applications. Temperature, resident time, concentration, and impregnation ratio, were the parameters used and ash content, carbon yield and surface area were the responses. The effect of preparation sequence was evaluated. The efficiency of the activated carbon on the adsorption of methanol was investigated an experimental rig. 100 g of sample was carbonized at 200, 400 and 600 ^oC, and the carbonized samples were used for solid adsorption refrigeration to determine the optimum carbonization temperature. Carbonization times (30, 60, 90, and 120 minutes), activating agent concentrations (25, 50, 75 and 100 %) and impregnation ratios (1:1, 1:2, 1:3, and 1:4 precursor to activating agents) at the optimum temperature were used to determine the optimum resident time, concentration and impregnation ratio. The results revealed that H_3PO_4 activated samples at optimum conditions of 500˚C temperature, 50 % concentration, 60 minutes resident time and 4 ml/g impregnation ratio yielded better response with low percentage of ash content (2.25 %), high carbon yield (73.63 %) and large surface area (2857.51 m^2/g) activated carbon were obtained at the optimum conditions. The adsorbing efficiencies of the carbons prepared through activation with H_3PO_4 achieved 0.084 and 14.5 of Coefficient of Performance (COP) and Specific Cooling Power (SCP) respectively. The results indicated that the carbon is activation before carbonization is well suited solid adsorption refrigeration applications.

Keywords: Activated carbon, adsorption refrigeration, Carbonization temperature, Coefficient of performance, Impregnation ratio, Resident time.

1. INTRODUCTION

Activated carbon (AC) is a generic term for a family of highly carbonaceous materials [1-5]. It is perhaps one of the most important types of industrial carbon materials and is prepared by carbonization and physical or chemical activation of a large number of raw materials of organic origin such as wood, coal, and lignite [6-10]. Characteristics of AC depend on the physical and chemical properties of the raw materials as well as method of activation [11-14]. The carbonization process enriches the carbon content and creates an initial porosity in the char while activation further develops the porosity and creates some array of the structure, thereby generating a highly porous solid as the final product [15-19]. One major advantage of naturally occurring organic substances as precursors for activated carbon is the possibility of producing a high-quality activated carbon with high percent yield when processed. This is actually impossible in the case of agricultural by-products because most of the biomass wastes have lower carbon content compared to the fossils fuel sources [20-24]. Industrially however, the cheap cost of raw material gives more significant impact as compared to the yield percent obtained. There have been significant increase technology requiring the use of activated carbons in a wide range of applications involving adsorption [25-29], with a corresponding increase in demand for adsorbents. Consequently, locally available carbonaceous materials have proven worthy for producing ACs. In search of alternative sources and cheaper carbons, agro wastes with average carbon content of 35 % have attracted the interest [2, 6, 16, 30].

Addressing climate change requires many solutions, with many of these solutions existing and centring on humans shifting the way of generating and consuming energy. The critical measures span through technologies that encourage less waste and smarter use of resources. Improvements to energy efficiency and pricing carbon are potent ways of reducing the quantity of carbon dioxide and other gases trapping heat on the planet. The exploitation of renewable energy offers a lot of outstanding benefits. A sustainable energy system may be regarded as a cost-efficient, reliable and environmentally one that effectively exploits local resources and production schemes [28, 31].

Thermally driven adsorption cooling cycles, popularly referred to as vapour adsorption refrigeration systems can be driven by low energy sources, such as industrial waste heat, solar systems etc. Apart from this, the system is relatively simple to construct, as it has no major moving parts. However, the heat source temperature can be further reduced as low as 50 °C [32-36].

AC is a proven and suitable adsorbent for solid adsorption refrigeration system when paired with an appropriate refrigerant. A challenge in activated carbon is to produce very specific carbons which are suitable for certain application. The most important characteristics of an activated carbon are the adsorption capacity and thermal conductivity which are highly influenced by source

materials and preparation conditions [37-42]. Thermal conductivity of adsorbent plays an important role towards improved performance of Adsorption Refrigeration System (ARS) in terms of Coefficient of Performance (COP) and Specific Cooling Point (SCP). The major challenge of activated carbon pair with refrigerant for ARS is poor thermal conductivity of the adsorbent that is usually close to those of insulation materials. Thermal conductivity of activated carbon is largely dependent on source material and activation conditions. These activation conditions directly influence the physical properties of the activated carbon. The activation conditions could be evaluated to obtain best production parameters for activated carbon that will be suitable for solid Adsorption Refrigeration System [43-46].

Activated carbon-methanol is one of the most promising working pairs in practical systems because of its large adsorption quantity and low adsorption heat (1800 to 2000 kJ/kg). Low adsorption heat is beneficial to the system's COP because the majority of heat consumption in the desorption phase is the adsorption heat. Another advantage of activated carbon-methanol is low desorption temperature (about 100 °C), which is within a suitable temperature range for using solar energy as a heat source [47-49]. Thus, the exploration of functional carbonaceous adsorbent materials such as Raffia endocarp activated carbon (REAC) paired with methanol for adsorption cooling/refrigeration applications could be beneficial in terms of COP [50].

Raphia palm is an evergreen palm with an un-branched stem up to 10 m tall topped by a crown of erect large leaves up to 12 m long each. The oily mesocarp is a laxative with stomachic properties and is used in traditional medicine and as an ointment for pains. In Nigeria, Raphia palms grow wild in the lowland forest region and swamps of the South as well as river courses of the Savannah region of the North. The economic importance of Raphia Africana fruits includes its oil which can be used for cooking and making of confectionery, the mature and ripe fruit served as food for coastal people of Katsina Ala local government of Benue state, Nigeria. It is also reported that the fruit contains plant growth regulators such as auxins, cytokinins, ethylene, gibberellins and other chemicals which can be used in tissue culture and also to stupefy fish [50-53].

Not many studies have been reported on converting Raphia nut endocarp into activated carbon for the purpose of adsorption refrigeration system experimentation. Akpen *et al.* [51] produced AC carbon from raffia nut for the purpose of coloring removal from waste water using chemical activation with $ZnCl_2$. They concluded that the best procedure for preparation is activation before carbonization. Elizalde *et al.* [52] produced AC from three source such as Guava seed, Avocado kernel and used commercial AC for removal of gadolinium-based contrast agents, chemical activation was used and a proposed method for elimination of GBCA from patient urine before its discharge into wastewater was arrived at. Kwaghger *et al.* [54] produced AC from Mango kernels and compared the isotherms for it with those of commercial activated carbon. Abdulrazak *et al.* [55] produced AC from African palm fruit for removal of heavy metals that have several components constituting high level of pollution to the environment. Pathania *et al.* [56] developed AC from *Ficus Carica bast* (FCBAC) using chemical activation for the purpose of methylene blue (MB) uptake by the FCBAC. A challenge in AC production is to produce very specific carbons which are suitable for certain applications. The most important characteristics of an activated carbon is its adsorption capacity which is highly influenced by the preparation conditions [57, 58].

At present, there is limited local technology available in the country for the preparation processing of activated carbons for adsorption refrigeration applications. Nigeria is among the world leaders in agriculture production. However, much of our produce goes waste due to absence of storage facilities like refrigeration system in the rural area where this production takes place. The solution to this problem lies in researching into the feasibility or otherwise of using local raw materials to develop adsorbents for adsorption cooling systems, which are much cheaper, simpler and easier to maintain. Raffia palm endocarp which are in abundance in some parts of Nigeria, most especially in Benue State in the North central part of the country have not been investigated as possible precursor for the production of activated carbons for solid adsorption refrigeration. Raffia palm endocarp is choosing for this study because of one important common ground about adsorbent from agricultural by-product which is the fact that they are waste by-product that always constitute disposal problem. Another advantage of this adsorbent production technique is the use of waste to preserve another agricultural product hence resulting to environmental sustainability, especially for the coastal part of Nigeria where the product is available in abundance and agriculture is the main economic activity [31]. The transformation of agricultural wastes into valuable end products may help to increase crop yields, create jobs and reduce solid waste disposal problems [32].

In the present study, the possibility of using Raphia nut endocarp as adsorbent source was explored using chemical activation and the best production parameters required to obtain adequate activated carbon with suitable properties in terms of carbon yield, surface area and ash content were also explored. The AC produced with the desired characteristics was compared with the commercial activated carbon through experimental test in an experimental rig to determine cooling effect/Specific Cooling Power (SCP) and Coefficient of Performance (COP).

MATERIALS AND METHODS

Matured Raphia palm nuts were collected from fresh water swamp forest of Shitile district of Katsina Ala local government area of Benue State. Samples were processed according to the procedure adopted by Walhof [59]. The sample fruit pericarp, mesocarp and endocarp were separated after which the endocarps were sun-dried for two weeks and then crushed with a 3 Hp nut cracker mill. The particles were sun-dried again for 5 hours to remove any residual moisture and sieved using sieve size of 600

µm (6 mm) for further experimentation. After impregnation for 24 hours, the samples were carbonized in a Carbolite- Model-GPC 12/81+103 furnace, rinsed, dried and crushed to obtain the desired particles that were passed through the sieve size of 300 µm (3 mm). The samples were stored in a moisture free containers for further experimentation [60].

Two activating agents, phosphoric acid (H_3PO_4) and calcium chloride ($CaCl_2$), were used to treat the Raphia nut seed prior to pyrolysis to further improve the porous properties of the AC. They were prepared in concentrations of 25, 50, 75 and 100 % to evaluate their effects, among other parameters, on the properties of the AC. H_3PO_4 was chosen as one of the reagents because of its ability to increase carbon content and reduce hydrogen and oxygen contents from carbon materials. The higher the concentration of H_3PO_4, the lower the hydrogen and oxygen content and the higher the carbon yield [61]. Kwaghger *et al.* [33] found that $CaCl_2$ generated better result than other reagents used for chemical activation of activated carbon from mango kernels which prompted its choice as the second activating agent for this study.

H_3PO_4 was prepared in four different concentrations of 25, 50, 75 and 100 % using distilled water. 25, 50 and 75 ml of the acid were added to 75, 50 and 25 ml of distilled water to obtain 25, 50 and 75 % by volume concentrations of acid activating agent. For 100 % volume concentration, no distilled water was added. In preparing the $CaCl_2$ into the concentrations studied, 25, 50, 75 and 100 g of the anhydrous salts were each added to 100 ml of distilled water to obtain 25, 50, 75 and 100 % concentration of the salt activating agent.

Four production parameters which are carbonization temperature, concentration of the activating agent, impregnation ratio of activating agent to Raphia fruit endocarp sample and resident time were studied because of their significance to the ash content, surface area and carbon yield [28]. Optimization with mathematical and statistical package (IBM SPSS Statistics Data Editor (Software) Version 23 and Excel Solver 2010) were applied in this work to study the effect of variables on ash content, carbon yield and surface area of the prepared ACs. This method is suitable for fitting a quadratic surface and it helped to optimize the effective parameters with a minimum number of experiments as well as analyze the interaction between parameters [58, 62].

Moisture content, ash content, bulk density, carbon yield and surface area were calculated using relevant equations based on proximate analysis of the product and relevant literature reviewed for the prepared AC. The moisture content was determined according to ASTM 2867-99. The weight of a dried crucible was recorded as W_1. Then 3 g of the sample was weighed into a pre-weighed crucible and the weight of both of the sample and the crucible was also recorded as W_2. The sample was dried at 115 °C in an electric oven with the crucible left opened in the oven for 2 hours, 2 minutes and the weights were recorded after the samples were allowed to cool until a constant weight was obtained. The moisture content was computed using equation 1 [63].

$$\text{Moisture Content } (\%) = \left(\frac{W_1 - W_2}{W_1} \times 100\right) \quad (1)$$

The Ash content was determined according to the ASTM D2866-94. The crucibles used were washed, dried in an oven and cooled in a desiccator. The weight of each crucible was recorded as W_1. Then 2 g of the sample was measured into the pre-weighed crucible and the weight of both the sample and the crucible were recorded as W_2. The sample was then heated at a temperature of about 750 °C in a muffle furnace with the crucible left opened for 58 minutes. It was then removed from the furnace, allowed to cool and the weight of the sample and the crucible after ash was recorded as W_3. The ash content for the sample was calculated using equation 2 [64].

$$Ash\ Content\ (\%) = \left(\frac{W_3 - W_1}{W_2 - W_1}\right) \times 100 \quad (2)$$

where W_1 = weight of the empty crucible, W_2 = weight of crucible + sample before heating, and W_3 = weight of crucible + sample after heating.

The bulk density was determined by steeping 3 g of uncarbonized sample into a 10 ml measuring cylinder which was then tapped on a table until it occupied a minimum volume. The apparent volume was taken at the nearest graduated unit. The bulk density was calculated in g/ml using equation 3.

$$Bulk\ Density, B_d = \left(\frac{M_2 - M_1}{V}\right) \quad (3)$$

where M_1 = mass of the empty measuring cylinder in grams, M_2 = mass of measuring cylinder + its contents, and V = volume of the measuring cylinder in litres.

The pH was determined using the following procedure. 1 g of carbonized carbon of the shell sample was measured into a conical flask and 100 ml distilled water was mixed with it. The mixture was vigorously agitated for an hour and then filtered. The pH of the filtrate was recorded using a pH meter [65].

The carbon yield was determined after sample processing in terms of raw material mass. The dried weight, W_{ca} (g) of each pre-treated sample was determined using a Mettler balance and the carbon yield calculated using equation 4.

$$Carbon\ Yield\ (\%) = \frac{W_f}{W_{ca}} \times 100 \quad (4)$$

W_f = dry weight of REAC and W_{ca} (g) = pre-treated sample used in the carbonization and activation processes.

The diameter assuming spherical shape of the REAC was obtained by passing the crushed carbon through sieve size of 3 mm and the external surface area was calculated using equation 5 [30].

$$Surface\ Area = \frac{6\ (\mathrm{m}^2/\mathrm{g})}{\mathrm{B_d P_d}} \quad (5)$$

where B_d = particle bulk density and P_d = the particle diameter.

Figure 1 shows a picture of the experimental rig for the solid adsorption refrigeration system. The design was done according to the procedure adopted by Kwaghger *et al.* [32] with some modifications in a view of achieving desired objectives. The system incorporates a combined one each of adsorber/generator, and a condenser, a control (capillary tube) and one evaporator integrating measuring devices for temperature and pressure. The experimental set up consists of two vessels, a spiral piped air cooled condenser, a vertical tube for conveying refrigerant vapour, 2 pressure gauges, 1 thermocouple, one control valves, 3 m length of high temperature fluid pipe (HTF) and an electric kettle. One vessel with implant of corrugated pipe wrapped with wire gauze acts as a combined adsorber/generator while the other vessel with coiled bundle of pipe served as an evaporator/receiver for storing the condensed methanol. During generation, the liquid refrigerant (methanol) was released from the AC as vapour and was condensed in the condenser tubes before metered by the capillary tube to the evaporator/receiver. Heating of the high temperature fluid was achieved by the use of electric kettle filled with water.

In order to improve the thermal conductivity of the adsorbent and enhancing the heat transfer properties of the bed, the adsorbent materials (REAC) was consolidated by compressing it mechanically into the shell. Additionally, a highly conductive compound (cerabol) and aluminum strips were incorporated in the adsorbent bed to further enhance the heat transfer within the adsorber shell. The evaporator is lagged with fibre glass and elastomeric thermal insulator (amarflex) to retard heat gain and control condensation drip from chilled water from the refrigeration system. Lagging of receiver/evaporator also guaranteed sustainable thermal efficiency.

The response of the control device was monitored by a counting down time switch calibrated in 12 hours. A fast response metering instrument (clinical thermometer, pressure gauge, and thermocouple) was used to measure the operating condition of the system. All modifications were aimed at enhancing accuracy of the readings. A capillary tube expansion device was employed as a refrigerant control device for the constructed test rig. The rig was used for determination of adsorption capacity of the activated carbon-methanol pair, refrigeration effect, and the COP. The system is capable of operating at temperature and pressure in the ranges of 25 - 120 °C and 0.5 - 7 bar respectively.

The leakages that may undermine the effectiveness of the system due to the thermal stresses were prevented by proper construction. A leakage testing procedure to ensure that change in atmospheric pressure does not affect methanol leakage at it is sensitive to changes in atmospheric pressure was carried out.

According to the Holdridge life zone system of bioclimatic classification, Makurdi is situated in or near the tropical dry forest biome and as such has average temperature of 27.6 °C. Condensing temperature of 28 ^{o}C was then selected as the average ambient temperature for the air cooled condenser for a typical Makurdi weather condition. The corresponding saturated pressure at this temperature was 0.17 bars [32].

Two similar vessels of aluminum were used as the adsorber/generator and evaporator/ receiver. They have maximum capacity of 2 liters to accommodate activated carbon- methanol, high temperature fluid pipe (hot water pipe) and desorbed methanol respectively. Weighing the evaporator/ receiver at the beginning and end of each test run gave the mass of methanol generated.

The generating temperature was between 100 to 120 ^{o}C and the corresponding pressure was 6.39 bars. Decomposition of methanol into other compounds such as diethyl ether occurs above the chosen temperature range. The vessels internal diameter, *d*, was chosen to be 100 mm. The minimum tensile strength of the aluminum alloy used, σ was 90 MPa [32].The wall thickness, *t*, was calculated from equation 6.

$$\sigma = \left[\frac{D^2 - d^2}{D^2 - d^2}\right]\frac{P}{2t} \quad (6)$$

where, σ = Tensile strength of material, *D* = outer diameter, *d* = internal diameter and *P* = system pressure.

From the calculated value t, the vessels outer diameter was to be 101 mm. Due to the difficulty in casting the vessel with this thickness, an outer diameter of 105 mm was selected giving the vessel a thickness of 5 mm. The capacity of the vessels was to be 2 liters (2000000 mm^3). So the height, *h* of the vessels was calculated using equation 7 from which *h* = 254 mm.

$$V = \frac{\pi d^2 h}{4} \quad (7)$$

A height of 255 mm was used and a rubber O-ring of diameter 100 mm was incorporated in the generator cover to make it air-tight. The same dimensions were used for the evaporator/receiver.

Assuming the maximum amount of methanol to be condensed as 50 g and a condensing time of 120 minutes, and the other operating conditions used were generating pressure = 6.39 bars, generating temperature = 120 ^{o}C, condensing temperature = 28 ^{o}C, mean ambient room temperature = 25 ^{o}C, tube internal diameter = 3.0 mm and tube external diameter = 6.35 mm. The mass flow rate of methanol, *m* was calculated as 6.944 × 10^{-6} kg/s from $m = \frac{mass}{time}$ b.

Literature suggests that both steel and copper are compatible with methanol for tubing. Copper tube was thus selected due to its low cost and availability. Estimating the length of the condenser tube requires considering the condenser as a heat exchanger

with hot fluid flows inside and a fluid of constant temperature (air) flowing outside it. A counter flow heat exchanger situation was assumed. The rate of heat loss from the fluid, Q was calculated from equation 8.

$$Q = UA\Delta T_{LMTD} = UA\left[\frac{\Delta T_a - \Delta T_b}{ln\left[\frac{\Delta T_a}{\Delta T_b}\right]}\right] \quad (8)$$

where U = overall heat transfer coefficient, A = cross- sectional area of condenser pipe, $\Delta T_{LMTD} = 26\,℃ = \frac{[T_{hin}-T_{cout}]-[T_{hout}-T_{cin}]}{ln\left[\frac{T_{hin}-T_{cout}}{T_{hout}-T_{cin}}\right]}$, T_{hin} = methanol inlet temperature (120 ^{o}C), T_{hout} = methanol outlet temperature (28 ^{o}C), T_{cin}= ambient air temperature at inlet section (25 ^{o}C) and T_{cout} = ambient air temperature at outlet section (25 ^{o}C).

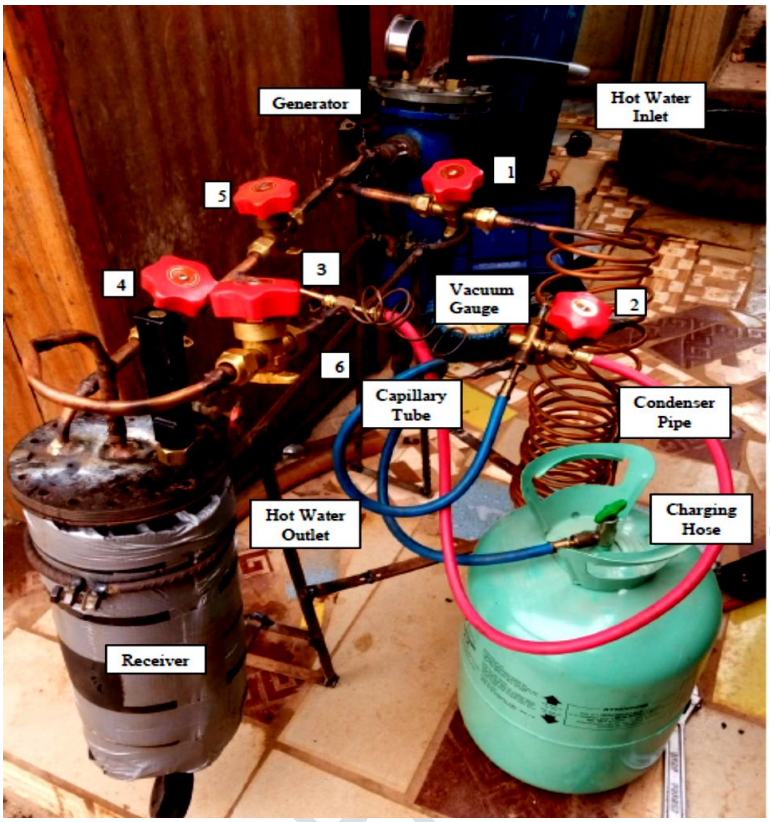

Fig. 1. Picture of the Experimental Rig for Solid Adsorption system

On the inside of the tube, heat transfer is by convection. The fluid properties change with changes in temperature but effective values could be estimated at arithmetic mean temperature, T_{am} of the methanol. Thus, $T_{am} = \frac{120+28}{2} = 78$ ℃. The pipe cross sectional area was calculated from the equation, $A = {\pi d^2}/{4}$ to be 7.06858 mm².

Reynolds number was calculated from equation 9, with the viscosity at 78 °C (351 K), $\mu = 280.5 \times 10^{-6} kg/m.s$ to be 10.51.

$$R_e = \frac{md}{\mu A} \quad (9)$$

Hence, the flow was laminar. Assuming the flow was fully developed, it has constant heat flux along the axial part of the wall and the pipe being circular then, the Nusselt number was constant to be 3.66 based on the aforementioned assumptions [66]. Then from equation 10, the convective heat transfer for methanol h_m can then be computed.

$$N_u = \frac{h_m d}{k_m} \quad (10)$$

The thermal conductivity of methanol, k_m at 78 ^{o}C is 0.1864 W/m^oC from where h_m = 227.40 W/m℃.

The heat transfer in the case of condensation at the outside wall of the condenser to ambient air was basically by free convection. For a horizontal pipe, equation 11 is applicable.

$$GrPr = \frac{a\beta(T_m - T_a)d^3}{\nu^2}Pr \quad (11)$$

where, Gr = Grashof number, Pr = Prandtl number, a = acceleration due to gravity, β = temperature coefficient of thermal conductivity given as $\beta = {}^{1}/_{T}$, T_m = temperature of methanol in tube, T_a = ambient temperature, d = diameter of tube and ν = kinematic viscosity and $T = ½(T_m + T_a) = ½(28 + 25) = 26.5\,℃ = 299.5\,K$ and $\beta = {}^{1}/_{299.5} = 3.34 \times 10^{-3}K^{-1}$. At this temperature, properties of air are $P_r = 6.66$; and $\nu = 0.685 \times 10^{-6}\,m^2/s$. It follows that $G_rP_r = 2.97 \times 10^6$. Now, $N_u = C(G_rP_r)^m$. The values of C and m are 0.53 and 0.25 respectively (Holman, 1979). So that $N_u = 22.002$. N_u was also calculated from equation 12, from which, $h = {}^{kN_u}/_{d}$.

$$N_u = \frac{hd}{K_a} \quad (12)$$

The thermal conductivity, k_a for air at 299.5 K is $0.0263\,W/mK$, so that $h_a = 90.72\,W/mK$.

The thermal resistance of aluminum wall material was neglected because of its high thermal conductivity. The overall heat transfer coefficient was calculated from equation13 to be $0.0625\,W/m^2K$.

$$\frac{1}{U} = \frac{1}{h_m} + \frac{1}{h_a} \quad (13)$$

The heat to be extracted from the hot methanol to cool from 120 °C to 28 °C was calculated from equations 14, 15 and 16.

$$q = UA\Delta T_{LMTD} \quad (14)$$

$$A = \frac{q}{U\Delta T_{LMTD}} \quad (15)$$

$$A = \pi dl \quad (16)$$

where l is the length of condenser tube $l = \frac{q}{\pi dU\Delta T_{LMTD}}$, $q = mc_{pm}(T_{in} - T_{out})$ and $c_{pm} = 192\,kJ/kgK$. Hence, the length of the tube, l was 1.96 m.

For methanol condensing at 28 °C, assuming laminar flow of condensate and that condensation was essentially film-wise. For a vertical tube, the Nusselt number was calculated from equation 17.

$$N_u = 0.9428\left[\frac{l_2^3\rho_f(\rho_f - \rho_g)g\{h_{fg} + 0.68c(\Delta T)\}}{\mu k(\Delta T)}\right]^{1/4} \quad (17)$$

The thermo physical properties of methanol at 301 K (28 °C) used were ρ_f = liquid density ($783.9\,kg/m^3$), ρ_g = vapour density ($0.329kg/m^3$), h_{fg}= specific heat of methanol ($1161.5\,kJ/kg$), μ = liquid kinematic viscosity ($401\times 10^{-6}\,Pa.s$), c = heat capacity ($2.554\,kJ/kgK$) and k_m= thermal conductivity ($0.193\,W/mK$). Thus, the condensing length wasl_2 = 7.688 mm. This implies that the condensing length was very small compared with the cooling length; a condensing length of 2 m was used.

The result of predictive equation derived from equation 18 as below is depicted in table 9, this is used to compare R^2 value for the treatment of samples with the activating agents ($CaCl_2$ and H_3PO_4).

$$\text{Dependent Variable} = \text{A} + (\text{B} \times \text{Temp}) + (\text{C} \times \text{Conc}) + (\text{D} \times \text{Time}) + (\text{E} \times \text{Ratio}) + \text{F} \times (\text{Temp}^2) + \text{G} \times (\text{Conc}^2) + \text{H} \times (\text{Time}^2) + \text{K} \times (\text{Ratio}^2) \quad (18)$$

The accomplishment of an adsorption/desorption refrigeration cycle relies upon the nature of the AC utilized. Also, performance declination can be attributed to the loss of vacuum in the system. The sensible heat of both the generator and the adsorbent was not to exceed 100 °C, as excessive heating would result in the decomposition of the methanol to dimethylether [67].To achieve this, the test rig was first pressurized by pumping through the vacuum valve/gauge to detect leakages. After this procedure, the system was evacuated through the same vacuum valve during which all other valves were opened. After evacuating the system, the valve was shut for the rest of the experiment. The vacuum pressure was recorded using the vacuum pressure gauge. In order to further analyze the characteristics of the REAC, it was necessary to measure desorption and adsorption characteristics of REAC- methanol pair and compare with the behavior with commercial activated carbon (CAC) - methanol pair known to be a suitable adsorbent, measure the refrigeration effect (or the cooling effect) and the COP [68].

As seen in Figure 3, the generator of mass 2300 g, embedded with corrugated high temperature fluid pipe, was filled with 250 g of AC and 250 g of methanol in the first instance (masses of both REAC and CAC were later varied). The water was heated using electric kettle with variable heat input control. Assuming full flow through the high temperature fluid pipe (HTF), the energy in the hot water flowing through the pipe increases the temperature and pressure of the system. During the refrigerant generation process (generator heated) the appropriate valves were also closed and then opened when the system pressure reached the condenser pressure and heating continued at that pressure till the concentration of the adsorbent reach the minimum level.

As heat was added, the increase in temperature of the generator and the weight of methanol generated were recorded at 15 minutes intervals. When the pressure of methanol in the generator reached desorption pressure, coinciding with increase in the receiver mass, the valve connecting the generator to the condenser was then opened for the methanol vapour to escape and be condensed. The desorbed refrigerant vapour then flows through the air cooled condenser pipe. The valves connecting the condenser to the control device (capillary tube) and evaporator/ receiver containing cooling coils were then opened to admit. The

process continued until the temperature of the adsorbent reached the desorption temperature of about 100 ^{o}C. The valves connecting the evaporator/receiver to the capillary tube and condensing pipe were then shut and that of the methanol vapour return line opened to allow the pressure of methanol drop. When the temperature of the adsorbent in the generator as well as the pressure of the methanol in the evaporator dropped, the adsorbent re-adsorbed the refrigerant. The system is intermittent as two or more adsorbers are required to make it continuous. For this reason, the adsorber needed to be cooled down to evaporator pressure for the purpose of re-adsorption of desorbed methanol. This was achieved by closing hot water inlet valve and opening of cool water inlet valve to run through the HTF. During the return cycle, the weight loss of the refrigerant as it evaporates, temperatures at generator and evaporator were measured every 30 minutes [47]. The cooling effect was obtained from refrigerant evaporation during the adsorption process as the temperature dropped. The produced REAC and the CAC were subjected through this experimental procedure with the mass of the REAC and CAC adjusted (250, 200, 150, and 100 g) to give initial adsorbent capacity of 1, 0.8, 0.6 and 0.4 g/g respectively.

Desorption and adsorption characteristics of REAC and CAC were analyzed and the cooling effect compared. Usually, the desirable characteristics of any cooling device are described by its cooling effect, the COP and its ability to exhibit desorption and adsorption equilibrium. The COP was calculated from the expressions in equations 18 - 20. The refrigeration effect is the difference between the initial temperature of water in the evaporator/ receiver and the temperature at the end of the adsorption process at the evaporator/ receiver [32, 46, 68]. According to Li *et al*. [44], equilibrium is established when the quantity of refrigerant desorbed equals the quantity re-adsorbed.

$$COP = \frac{Q_c}{Q_{in}} \tag{18}$$

where the useful cooling of adsorbent, Q_c and the heating output per kilogram of adsorbent, Q_{in}were calculated from equations 19 and 20 respectively.

$$Q_c = L(\Delta x) - C_{pm}(T_{a1} - T_{a2}) \tag{19}$$

$$Q_{in} = Q_{sen} + \Delta H \tag{20}$$

The sensible heat, Q_{sen} in equation 20, can be calculated from equation 21.

$$Q_{sen} = m_w C_{pw}(T_i - T_f) \tag{21}$$

IBM SPSS statistic 23 (2015 version) software package was used to analyze the results. It is a collection of mathematical and statistical techniques that are useful for modeling and analyzing problems in which a response of interest is influenced by several variables [69, 70].

The effect of preparation variables temperature, concentration, impregnation ratio and resident time on surface area, carbon yield and ash content of the produced AC were investigated. ANOVA at 95 % confidence level was used to identify which factor(s) or their interactions in the models were significantly contributing to obtaining a particular response. Excel 2010 solver for Response Optimizer was used to determine the right settings for optimal results. GRG (generalize Reduced Gradient) design was adopted because the regression equation of best fit was non-linear. Local optimum solution was found. The value of model terms where P-value is less than 0.05 or where F-value is greater than F-critical indicates that the model terms were significant and there is synergetic relationship between the factors. Checking the adequacy of the model is an important part of data analysis procedure, since it would result in poor or misleading results if the fit is inadequate. Cell mean plots were used to validate the ANOVA result for combinations of different factors on responses.

Texture and surface properties of the adsorbents play an essential role in determining their performance and the final application of carbon materials. Characterization of REAC by Scanning electron microscopy was conducted to study its surface topography. A Scanning Electron Microscope with high magnifications (BRUKER 125ev model) was used to characterize surface properties of the REAC under optimized condition.

RESULTS AND DISCUSSION

Table 1 shows the phytochemical analysis of raffia nut endocarp carried out in the laboratory of department of agronomy, Federal University of Agriculture (now Joseph Sarwuan Tarka University), Makurdi. The results indicate the suitability of the material for AC production [10, 54].

The experimental response varied between 67.00 - 1.0 % ash content, 64.59 - 891.71 m^2/g surface area and 38.10 - 78.90 % carbon yield for $CaCl_2$, and 50.18 - 0.22 % ash content, 387.80 - 4000.0 m^2/g surface area and 55.48 - 82.10 % carbon yield for H_3PO_4. These results were obtained at various temperatures (200, 400 and 600 °C), resident time (30, 60, 90 and 120 minutes), concentration (25, 50, 75 and 100 %) and impregnation ratio (1, 2, 3 and 4). The responses fall within acceptable range for adsorption application [4, 58]. In order to determine the best experimental conditions for maximum output of the REAC, the obtained results were further exploited using Excel 2010 solver response optimizer to determine which factor(s) or their interactions was significant or had greatest or least effect on the responses investigated, and at what point the variation of the studied variables will give maximum requirements of a good adsorbent. Table 2 show Spearman's correlation table showing p-values to test the effect of individual input parameters over the output parameters according to the treatment with the activating agents. $P < 0.05$ denotes significant effect. Table 3 shows spearman's correlation to test of treatments on the outputs.

Table 1. Phytochemical Analysis of Raffia Nut Endocarp

Parameters	Values
Ash content (%)	2.74
Moisture content (%)	10.24
Crude Fibre (%)	23.28
Crude Protein (%)	11.38
Fat/Oil (%)	1.85

Table 2. Spearman's Correlation Showing p-values (0.5 level) to test the effect of input Parameters over the output Parameters based on treatment with the Activating Agents.

	$CaCl_2$ Activated Samples			H_3PO_4 Activated Samples			Combined Treatments		
	Ash	**SA**	**CY**	**Ash**	**SA**	**CY**	**Ash**	**SA**	**CY**
T	0.706	0.341	0.053	0.928	0.000	0.505	0.841	0.000	0.321
C	0.672	0.000	0.254	0.795	0.791	0.000	0.575	0.136	0.047
Ti	0.000	0.000	0.717	0.995	0.812	0.000	0.000	0.000	0.008
R	0.768	0.756	0.000	0.792	0.072	0.975	0.968	0.720	0.000

Table 3. Spearman's Correlation for Testing of Treatments on the outputs (p-values at 0.5 level of significance)

	Ash Content	**Surface Area**	**Carbon Yield**
Treatments	0.560	0.000	0.000

The regression equations developed using code units for all the activating agents are presented in Table 4 for ash content, surface area and carbon yield with their correlation coefficient (R^2). The R^2 describes the amount, in percentage, of the total variation in the observed responses (ash content, surface area and carbon yield) that was attributed to the experimental variables (temperature, carbonization time, impregnation ratio and concentration of activating agent) studied. The positive sign in front of all terms in the models indicates a synergistic effect, whereas negative sign indicates antagonistic effect (IBM SPSS statistic 23, 2015 version). The ash content, surface area and carbon yield were utilized in the quadratic model according to the propositions of the software. The adequacy of the developed models was justified through the cell-mean-plot some of which are shown in Figures 5-18.

The model equations for ash content are shown in Table 4 for $CaCl_2$, H_3PO_4 and combined treatment. H_3PO_4 show very weak R^2 value for ash content (~ 26 %), indicating that only 26 % of the variation in ash content was explained by the model for H_3PO_4. For $CaCl_2$, resident time and impregnation ratio had antagonistic effect on the ash content while temperature and concentration had synergistic effect on the ash content. This was because resident time and impregnation ratio have negative coefficient while temperature and concentration have positive coefficient. The highest effect was from resident time with a coefficient of +1.445 for H_3PO_4, and only concentration had synergistic effect on ash content. Temperature, resident time and impregnation ratio had antagonistic effect on the ash content of the REAC. Here also, of the studied factors, combined treatment had the highest contribution to the ash content with a coefficient of $+1.085 \times 10^7$. The R^2 value for $CaCl_2$ was however higher (66.5 %). Time and concentration were the independent variables that had significant contributions to ash content of all the studied factors using $CaCl_2$. However, impregnation ratio and concentration have synergistic contribution to ash content. Impregnation ratio was the highest factor contributing to the ash content with a coefficient of -2.304. The studied factors however contributed more than their interaction. This could be why higher R^2 values were observed for $CaCl_2$. The low R^2 value of 26 % for H_3PO_4 could be due to the fact that the ANOVA for ash content of these activating agents indicate that most of the studied parameters were significant to the ash content of the REAC. For H_3PO_4, temperature and concentration were significant with p - values of 0.001 and 0.005 respectively. The contribution of the quadratic effect of temperature was negative for H_3PO_4 and positive for $CaCl_2$. This observation could be due to the fact that H_3PO_4 have very poor ash reducing ability while $CaCl_2$ is generally good in that [4].

Table 4. Predictive Equations for Ash Content, Surface Area and Carbon Yield for $CaCl_2$ and H_3PO_4.

Parameters	**Activation Method**	**Linear Models**	**R^2**
Ash Content	$CaCl_2$	$31.285 + 0.023T_P + 0.516C_X - 0.399T_m - 2.304R_T - 0.004{C_X}^2 + 0.497{R_T}^2$	0.665
	H_3PO_4	$-7.236 \times 10^7 - 0.105T_P + 0.318C_X - 0.272T_m - 0.429R_T + 1.085 \times 10^8 T_R - 0.002{C_X}^2 + 0.001{T_m}^2 + 0.079{R_T}^2 - 3.618 \times 10^7 {T_R}^2$	0.255

	Combined Treatment	$53.3 - 0.232T_P + 0.212C_X - 0.146T_m + 1.445R_T - 0.001{C_X}^2 + 0.001{T_m}^2 - 0.339{R_T}^2$	0.236
Surface area	$CaCl_2$	$-7.236 \times 10^7 - 1.99T_P - 0.584C_X - 0.133T_m + 42.989R_T + 1.085 \times 10^8 T_R - 0.006{C_X}^2 - 0.005{T_m}^2 + 3.869{R_T}^2 - 3.618 \times 10^7 {T_R}^2$	0.275
	H_3PO_4	$928.570 - 0.121T_P - 5.45C_X - 2.877T_m - 0.478R_T + 0.038{C_X}^2 + 0.01{T_m}^2 + 0.607{R_T}^2$	0.599
	Combined Treatment	$2286.588 - 3.858T_P + 4.282C_X + 2.611T_m + 86.458R_T + 0.001{T_P}^2 - 0.027{C_X}^2 - 0.019{T_m}^2 + 7.132{R_T}^2$	0.685
Carbon yield	$CaCl_2$	$22.137 + 0.108T_P + 0.11C_X - 0.14T_m + 4.089R_T - 0.001{C_X}^2 + 0.001{T_m}^2 + 0.326{R_T}^2$	0.528
	H_3PO_4	$46.218 + 0.034T_P + 0.067C_X + 0.130T_m + 5.055R_T - 1.014{R_T}^2$	0.258
	Combined treatment	$-7.236 \times 10^7 + 0.071T_P + 0.088C_X - 0.005T_m + 4.572R_T + 1.085 \times 10^8 T_R - 0.344{R_T}^2 - 3.618 \times 10^7 {T_R}^2$	0.541

T_P = Temperature; C_X = Concentration; T_m = Time; R_T = Ratio; T_R = Treatment

The model equations for surface area for the two activating agents are also shown in Table 4. The R^2 values for surface area of the studied activating agents were in the range of 28-68%. H_3PO_4 had the highest R^2 value of 68.5 %. From the Table 5, the t-Test of difference between the measured outputs according to treatment with $CaCl_2$ and H_3PO_4, all the studied variables significantly contributed to the surface area of the REAC, since all studied factors have p-values > 0.05. For H_3PO_4, Impregnation ratio had the highest effect and synergistic on the surface area with a coefficient of 86.46. Impregnation ratio was also reported to be a dominant factor responsible for surface area. The effects of concentration, resident time, and impregnation ratio were however synergistic while temperature remains the only factor with antagonistic effect. The model equation for $CaCl_2$, suggested that all the studied factors had antagonistic effect on the surface area than their interaction with concentration having the highest effect on the surface area with a coefficient of -5.45. This observation was consistent with those of Yorgum and Yildiz [71] and Shamsuddin *et al.* [72].

The model equation for carbon yield for the activating agents used are shown in Table 4. The R^2 values for the models equations for carbon yield range from 26 to 54 %. The model for $CaCl_2$ suggests that impregnation ratio was the highest factor contributing to the carbon yield with a coefficient of 4.089. All the factors apart from resident time had synergistic effect on the carbon yield. The effect of resident time suggests that as the resident time of $CaCl_2$ increases, the carbon yield decrease. The R^2 value was 53 % which was better than H_3PO_4 (26 %). All the independent variables studied had effect on the carbon content of the REAC. All variables studied had effect on the carbon content of the REAC and synergistic to the carbon yield as observed with H_3PO_4. Also, impregnation ratio had dominant effect on the carbon yield. Tan *et al.* [57] reported that temperature had a highly negative influence on the carbon yield compared with other factors, reporting an R^2 value of 95.7 %. The discrepancies observed could be due to the type of activating agent used and the nature of the activation used.

The ANOVA for ash content using H_3PO_4 suggests that concentration and temperature played decisive roles in the ash content of REAC (F- value = 171.21215). This observation was noted both at the linear and quadratic levels of the model (p-values of 0.000 and 0.000 respectively), that the p-values for concentration and temperature were 0.000 and 0.048 respectively. The interaction terms in the model were also significant. The interaction effect between temperature and concentration was observed to be highly significant (p-value of 0.000 < 0.05) as well as that of temperature and time with p-values of 0.000. This observation indicates that the effect of temperature on ash content was due to the concentration of H_3PO_4 as well as the resident time.

Table 5. T-Test of difference between the Measured Outputs According to Treatment with $CaCl_2$ and H_3PO_4

	$CaCl_2$		H_3PO_4		Combined Treatments	
	P-value	t-value	P-value	t-value	P-value	t-value
Ash	0.000	18.506	0.000	19.770	0.000	26.513
Surface Area	0.000	80.003	0.000	28.435	0.000	31.636
Carbon Yield	0.000	76.658	0.000	152.590	0.000	113.141

The ANOVA for ash content using $CaCl_2$ suggests that the model was significant. However, only the quadratic and the interaction terms of the model were significant (p-values of 0.000). The interaction effects between temperature and concentration as well as that of concentration and impregnation ratio were significant (p-values of 0.007 and 0.001 respectively).

All the factors studied were not linearly significant to the ash content of the REAC using $CaCl_2$ (p-values > 0.05). The quadratic effects of temperature and time were significant (p-values of 0.000 and 0.033 respectively). The quadratic effect of temperature played a decisive role in the ash content of the REAC (F- value = 126.00). The interaction effect between temperature and concentration as seen in the ANOVA for ash content using $CaCl_2$ was highly significant (p-value of 0.007). This suggests that the effect of concentration on the ash content depends on the carbonization temperature.

The ANOVA for carbon yield of REAC produced using $CaCl_2$ suggests that the model is significant at all levels (linear, quadratic and interaction) having p-values of 0.000. The interaction effect between temperature and time is highly significant with a p-value of 0.000 suggesting that the effect of temperature on carbon yield depends on the resident time. Temperature and concentration have significant quadratic effect on carbon yield having p-values of 0.000 and 0.005 respectively. The ANOVA for carbon yield using $CaCl_2$ indicates that out of the studied parameters, temperature and time contributed predominantly to surface area of the REAC.

The ANOVA for carbon yield using H_3PO_4 suggests that the model is significant as well as the linear, quadratic and interaction terms in the model (p-values of 0.000). The interaction effects between temperature and time, concentration and time as well as concentration and impregnation ratio were significant (p-values of 0.000, 0.013 and 0.044 respectively). The interaction effect between temperature and time suggests that the effect of temperature on the carbon yield depends on the resident time. The linear relationship of resident time with the carbon yield is significant (p-value of 0.000). Also, the ANOVA for carbon yield shows that resident time contributed decisively to carbon yield. The coefficient for resident time in the equation is positive (3.4286). These observations indicate that carbon yield increases linearly as the resident time increases. The interaction effects between concentration with resident time and impregnation ratio suggest that the effect of concentration on carbon yield was as a result of resident time and impregnation ratio. The trend observed with impregnation ratio using H_3PO_4 could be due to the fact that it promotes the oxidation process, therefore with high impregnation ratio, the gasification of surface carbon atoms was the predominant reaction, leading to increase in weight loss of carbon [73, 75].

Figures 2 to 7 show the effect of resident time, impregnation ratio and concentration on the ash content of the AC for the two activating agents. Figure 2 shows that the ash content generally reduced with increasing resident time for the $CaCl_2$ activating agent which is to be expected. It also shows that the reduction is less drastic for the lower temperatures. The Figure indicates that ash content decreases as the resident time increases. This observation was however noticed at carbonization temperatures of 200 and 400 °C only. Hesas *et al.* [75] stated that it is not necessary to prolong activation time beyond the basic requirement as doing so would cause pores enlargement that may collapse into ash, which may be undesirable depending on the requirements of the application. This observation could be due to the fact that diluting the concentration of H_3PO_4 could reduce its ash reducing ability. Typical ash content values of a good activating agent were observed at 100 % concentration with all p-value of almost (0.000). Figure 3 also shows a general decrease in the ash content with resident time for H_3PO_4. 50% concentration exhibited highest ash content [76]. However, the reduction curves were generally dispersed for the lower resident times and more clustered as at higher values. The figure shows the effect of concentration on the ash content at the studied temperatures; it shows that at 200 °C, ash content decrease with increase in concentration. At higher temperatures, 400 and 600 °C, concentration shows no effect on the ash content.

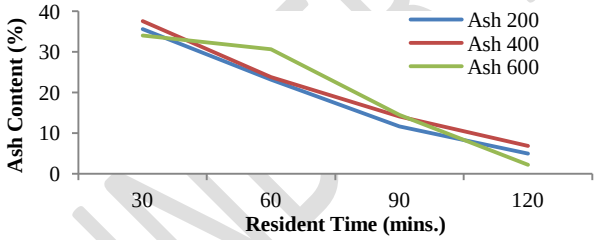

Fig. 2. Effect of Resident Time on Ash Content at a studied Temperature using $CaCl_2$.

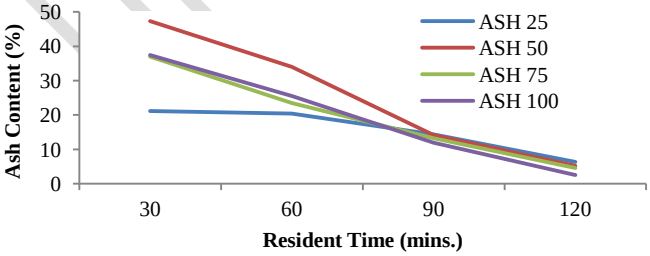

Fig. 3. Effect of Resident Time on Ash Content using H_3PO_4 for the various Concentrations.

Figures 4 and 5 show that the effect of impregnation ratio on ash content for the two activating agents is generally uniform with some fluctuations. They also show that temperature had a more profound effect on the ash content for the H_3PO_4 activated carbon than the one for $CaCl_2$ [77].

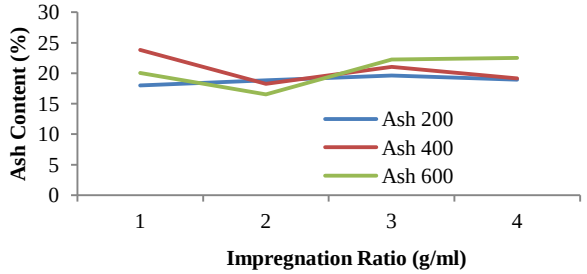

Fig. 4. Effect of Impregnation Ratio on Ash Content at a Studied Temperature Using $CaCl_2$.

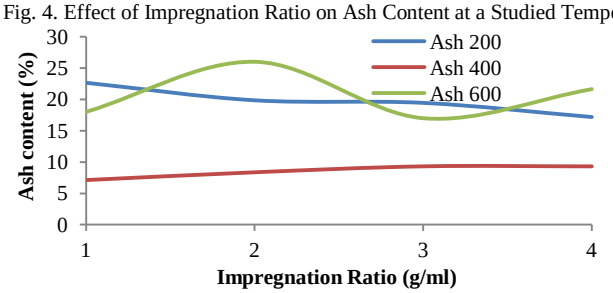

Fig. 5. Effect of impregnation ratio on ash content at a studied temperature using H_3PO_4.

Figures 6 and 7 show the effects of concentration on ash content for the activating agents at the various temperatures. For both of them, higher temperatures and increasing concentration favoured increase in ash content [58]. For $CaCl_2$, the value ash content actually reduced with concentration for 200 °C.

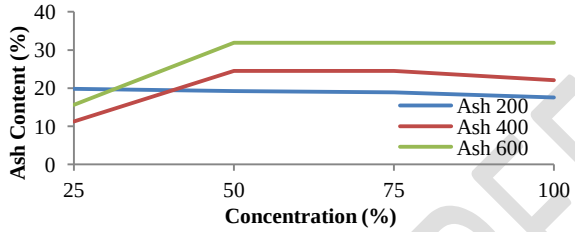

Fig. 6. Effect of Concentration on Ash Content at a Studied Temperature using $CaCl_2$.

Figures 7 to 10 show the effects of some of the parameters on the surface area of the AC. Figures 7 and 8 show the effect of resident time on surface area of the AC activated using the two agents at the different temperatures. For the $CaCl_2$ AC in Figure 7, surface area generally decreased with increasing resident time for all the temperatures due to the increase thermal stress within the material. For H_3PO_4 AC, however, the surface area did not change appreciably with increasing resident time as shown in Figure 9. However, the mean surface area was smallest for the highest temperature (600 °C) and highest for the medium temperature (400 °C), indicating that this activating agent aided the production of a more stable AC [9, 55].

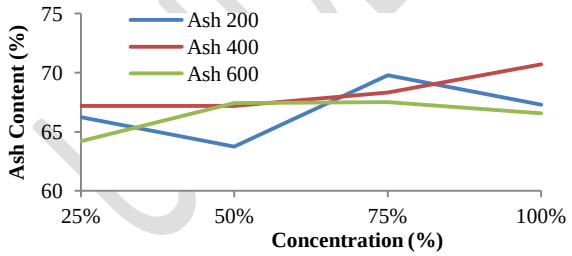

Fig. 7. Effect of Concentration on Ash Content at a studied temperature using H_3PO_4.

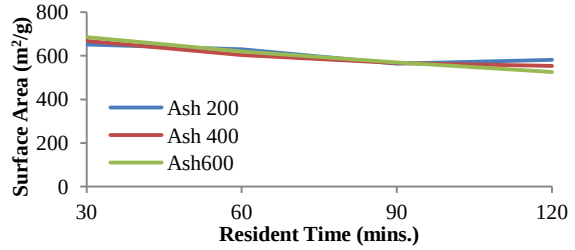

Fig. 8. Effect of Resident Time on Surface Area at different Temperatures using $CaCl_2$.

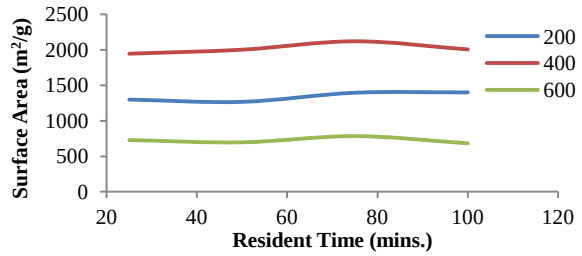

Fig. 9. Effect of Resident time on Surface Area at a Studied Temperature using H_3PO_4.

Figures 10 and 11 show the effect of impregnation ratio on the surface area of the AC for the two activating agents. In Figure 10, the effect was studied at different concentrations and it shows that the variation of the response with impregnation ratio was not significantly dispersed, indicating that at the various concentrations the surface area was reasonably constant. 25% concentration produced the higher limit of the surface area and 50% the lower one showing a relationship that is not specifically fits any trend based on the concentration for the $CaCl_2$ AC. This means that the combination of concentration and impregnation ratio do not affect surface area distinctly [21, 22]. Figure 11 shows the effect of the ratio on surface area for the AC activated with H_3PO_4 at the temperatures studied. For 200 °C, the surface area increased with impregnation ratio after an initial constant stretch up to about a ratio of about 2 before increasing more drastically for higher ratios. Also, the area was highest for this temperature and lowest for 600 °C, and the medium value at 400 °C. Hence, the lower temperature and increasing impregnation ratio favours the provision of larger surface area for the AC [39, 61].

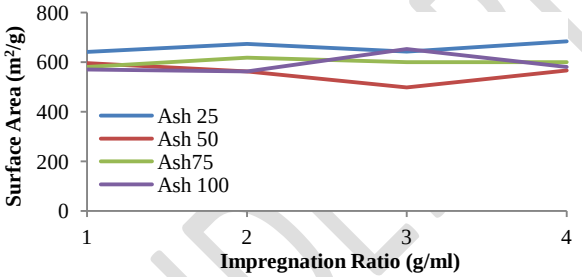

Fig. 10. Effect of Impregnation Ratio on Surface Area at a Studied Concentration using $CaCl_2$.

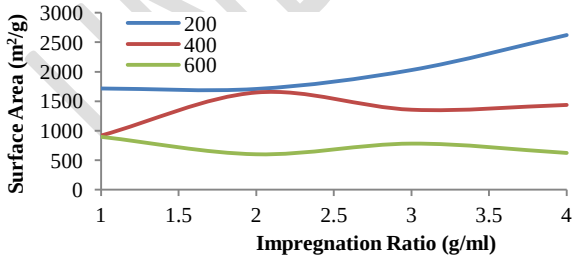

Fig. 11. Effect of Impregnation Ratio on Surface Area at a Studied Temperature using H_3PO_4.

Figures 12 to 15 show the effect of some of the parameters on carbon yield. Figure 12 shows the effect of resident time on the carbon yield of REAC using $CaCl_2$ at the temperatures studied, it can be seen that carbon yield increases as the resident time increases. This was noted mostly at temperatures of 400 and 600 °C while at 200 °C, the effect of time on carbon yield was

almost negligible. This observation was not consistent with the results of Zhang *et al.* [8]. They reported that carbon yield decreased with increasing resident time, and temperature. However, they used coconut husk-based and oil palm fibre-based activated carbons. In the present study, temperatures of 400 and 600 °C favoured higher carbon yield at increasing resident time. The discrepancies between their observation and the present study could be due to the fixed carbon and lignocellulosic composition of the starting materials used. Koehlert [26] reported that materials with higher carbon content should be volatilized to a much lesser extent to avoid carbon burn-off. High surface area is most important for activated carbons, however high carbon content is desired to achieve this high surface area [65].

Figure 13 shows that for the REAC using H_3PO_4, the same trend was observed up to around 60 to 80 minutes resident time. From that range however, the increase was observed for 400 and 200 °C carbonization temperature, while a decrease was observed for 600 °C with increasing resident time. Also, at the lower resident periods, the carbon yield was highest for 600 °C and fairly steady while it commenced steady increment for 400 and 200 °C. On the whole, the increment for 200 °C temperature was more linear than the others signifying a more a more straightforward interaction under those conditions [22, 77].

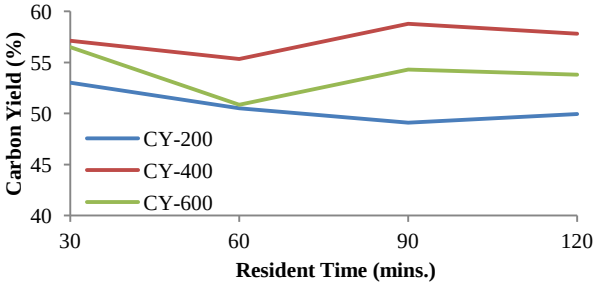

Fig. 12. Effect of Resident time on Carbon Yield at the Studied Temperature using $CaCl_2$.

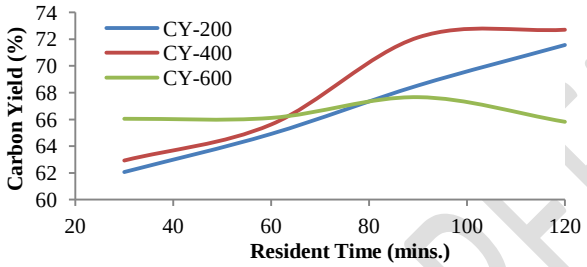

Fig. 13. Effect of Resident Time on Carbon Yield at a Studied Temperature using H_3PO_4.

Figure 14 depicts the influence of impregnation ratio on the carbon yield of the REAC produced with $CaCl_2$ at the various carbonization temperatures. The variation at 200 °C was literally constant probably due to inadequacy of the thermal environment to produce significant change in carbon generation. At the higher temperatures of 400 and 600 °C, carbon yield increased steadily with impregnation ratio with the carbonization temperature of 400 °C yielding the highest carbon content agreeing with the fact that though adequate thermal environment is needed, continual temperature increase is not necessary [58, 75].

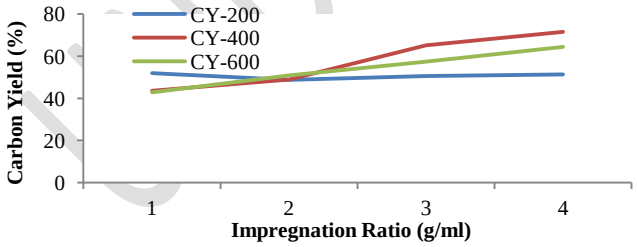

Fig. 14. Effect of Impregnation Ratio on Carbon Yield at the Studied Temperature using $CaCl_2$.

Figure 15 shows the effect of impregnation ratio on carbon yield for the various concentrations of the REAC produced with H_3PO_4. There was a general increase in carbon yield with increasing impregnation ratio without significant difference between the values for the respective concentrations indicating that there was no significant contribution by this parameter to the interaction between impregnation ratio and carbon yield [10, 22].

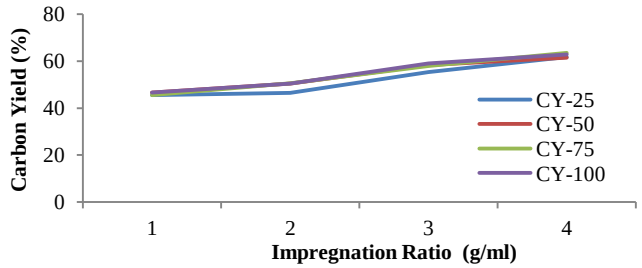

Fig. 15. Effect of Impregnation Ratio on Carbon Yield at the Studied Concentration using $CaCl_2$.

The result of the response evaluation analysis using the two activating agents are shown in Tables 6 and 7. The results indicate the optimum conditions at which the study could be set. The results also indicate that for the production process of REAC using H_3PO_4 to meet the desired quality, these conditions should be met. This will result in products with the characteristics shown in Table 7. All responses fall within acceptable boundaries. The results compared favourably with the reports of Hesas *et al.* [75], Karthikeyan *et al.* [4] and Sahu *et al.* [58]. The result suggests that H_3PO_4 have high ash reducing ability over the other activating agent used. The results of the response analysis for $CaCl_2$ are also shown in the Tables indicating the optimum conditions, within the limits of the study, at which desirable products could be achieved and the characteristics of the of the products as well as the individual desirability respectively.

Table 6. Evaluated Preparation Conditions from Excel Solver

Activating Agent	Temp (^oC)	Conc. (%)	Time (mins.)	Impregnation Ratio (ml/g)
$CaCl_2$	440	25	60	1
H_3PO_4	500	50	60	4

The result indicates that for production of REAC using $CaCl_2$ to meet the requirements of good adsorbents for adsorption refrigeration application. The optimal conditions reported by Kwaghger *et al.* [40] were 500 °C temperature, 60 minutes time and 4 g/g impregnation ratio. This resulted in carbons with surface area of 1141 m^2/g and carbon yield of 17.96 %. The temperature, impregnation ratio and time were higher than that obtained in this study using $CaCl_2$.

The SEM images of the REAC produced from the two activating agents used (H_3PO_4 and $CaCl_2$) are shown in Figure 16. They show that the activation stage produced extensive external surfaces, smooth but irregular cavities and pores. Also revealed is the fact that the activated carbon from H_3PO_4 has more desirable pore volume for refrigeration applications compared to the one activated with $CaCl_2$ [54]. This is shown in Figure 17.

Table 7. The Responses at Optimal Production Conditions

Activating Agent	Ash Content (%)	Surface Area (m^2/g)	Carbon Yield (%)
$CaCl_2$	6.00	698.91	53.13
H_3PO_4	2.25	2857.51	73.63

The efficiency of an adsorption/desorption refrigeration system is influenced by the choice of adsorbent/adsorbate pair. To further analyse the performance characteristics of the developed REAC- methanol pair, it was necessary to measure the desorbing and adsorbing characteristics of the pair, the refrigeration effect, the COP and compare with the CAC- methanol pair adjudged to be suitable for refrigeration purposes as reported by Li *et al.* [64].

Generally, the characteristics of an adsorption refrigeration system are described by the refrigeration effect (cooling effect in the evaporator) and the COP [64]. The refrigeration effect achieved was the reduction of the initial temperature of water of mass 500 g from 28-14, 28-14, 28-14 and 28-13.5 °C for REAC and from 28-15, 28-15, 28-15, and 28-14.5 °C for CAC at the studied adsorbent capacities. This low cooling effect could be attributed to the fact that the quantity of methanol desorbed was not significant to cause ice production. Ullah *et al.* [48] reported that the quantity of ice production (cooling effect) depends to a large extent on the quantity of desorbed refrigerant.

Figures 18 to 21 compare the refrigeration effects of REAC and CAC at different initial adsorbent capacity (1.0, 0.8, 0.6 and 0.4 g/g). It could be seen that REAC achieved lower value of refrigeration effect (13.5) compare to CAC (14.5) at 0.4 initial adsorbent capacity respectively. The reason for this desirable performance of REAC could be traced to its improved preparation conditions tailored towards a specific purpose for preparing REAC which is mainly for solid adsorption system. The result compared favourably with Kwaghger *et al.* [32] where refrigeration effect of 15.5 was achieved at 0.4 initial adsorbent capacity.

The COP is the amount of cooling achieved by a refrigeration machine per unit of heat supplied. The COP for the REAC was 0.084, 0.051, 0.038 and 0.041, while that of CAC was 0.0782 0.038, 0.026 and 0.023 at 1, 0.8, 0.6 and 0.4 g/g initial adsorbent

capacities respectively as seen in Table 8. This range was indeed close and could obviously be due to the fact that REAC and CAC have common desirable characteristics such as surface area and carbon yield. This could also be due to the fact that REAC and CAC have affinity for methanol [78, 79]. It was however observed that the COP of REAC is slightly higher than that of CAC at all the initial adsorbent capacities investigated. This could be due to the fact that the REAC has higher surface area and lower ash content (2857.51m^2/g and 2.25 %) than the surface area and ash content of CAC (950 - 1500 m^2/g and 3 %). The COP obtained in the study compared favorably with that obtained by Saha *et al.* [40] and Saha *et al.* [41] who used for solar sorption refrigeration with different adsorption pair. They were able to achieve the COP of 0.13 and 4.5 of ice produced. Boubakri *et al.* [80] achieved COP of 0.15 and an ice production of 4 kg using Activated carbon-Methanol pair for a solar power adsorption ice maker.

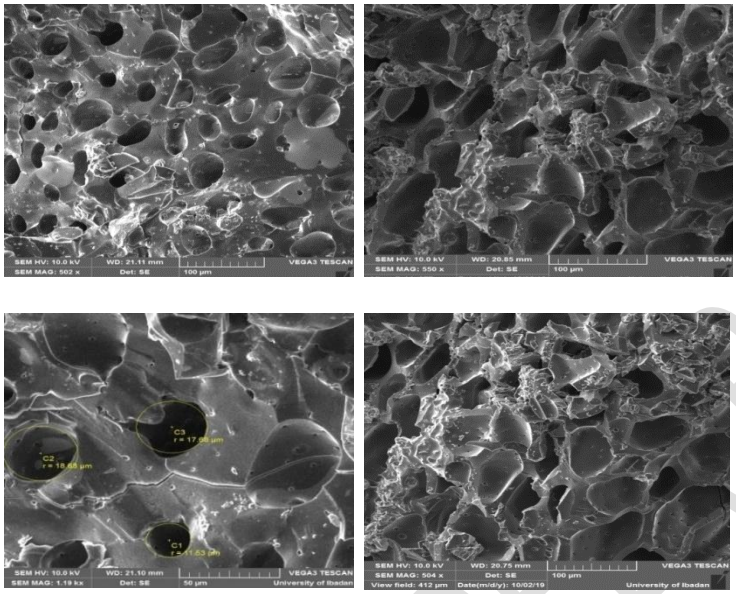

Fig. 16. SEM Micrograph for REAC produced under Optimum Condition to show Surface Morphology.

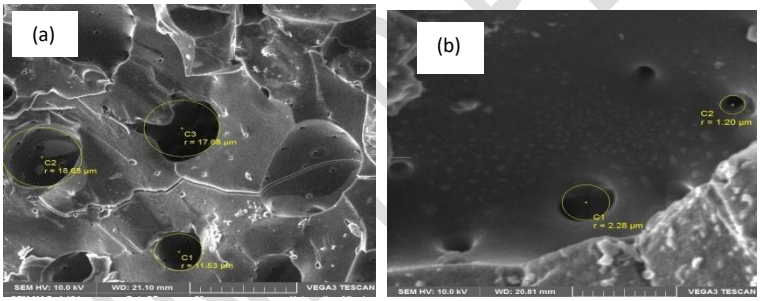

Fig. 17: SEM Micrograph showing Internal Radius of the Pore Cavity REAC produced with (a) H_3PO_4 and (b) $CaCl_2$.

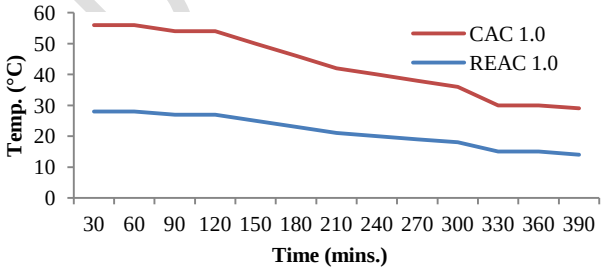

Fig. 18. Refrigeration effect for REAC and CAC at initial Adsorbent Capacity of 1.0.

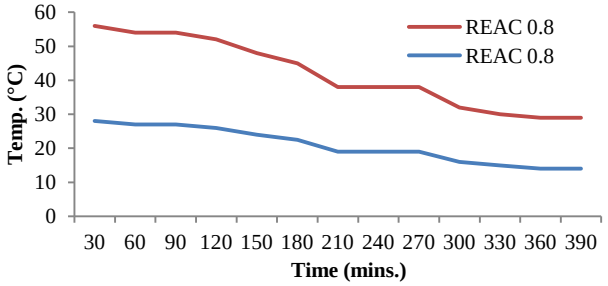

Fig. 19. Refrigeration effect for REAC and CAC at initial Adsorbent Capacity of 0.8.

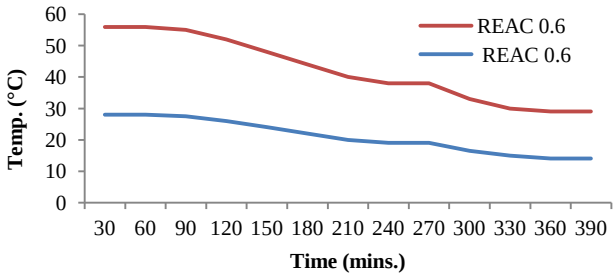

Fig. 20. Refrigeration effect for REAC and CAC at initial Adsorbent Capacity of 0.6.

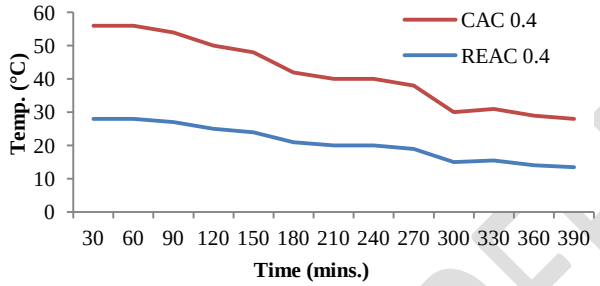

Fig. 21. Refrigeration effect for REAC and CAC at initial Adsorbent Capacity of 0.4

Table 8. Coefficient of Performance for the Adsorption Refrigeration at the Studied Adsorbent Initial Capacities.

Activated Carbon	**Coefficient of Performance**			
	1.0	**0.8**	**0.6**	**0.4**
REAC	0.084	0.051	0.038	0.041
CAC	0.082	0.038	0.026	0.023

CONCLUSIONS

The best production parameters for REAC was obtained when H_3PO_4 was used as activating agent at carbonization temperature of 500 ºC, 50 % concentration, 60 minutes resident time, and impregnation ratio of 4 ml/g. The COP evaluated for REAC- methanol was better than that obtained for CAC- methanol at the studied adsorbent capacities because chemical method was adopted for production of REAC and specifically for solvent recovery while common CAC usually produced through physical activation and most times not for solvent recovery. The refrigeration effect at the studied adsorbent capacities were low, suitable only for chilled water. Further studies to evaluate the best production parameters for activated carbon from Raphia nut endocarp are envisaged specifically for solid adsorption refrigeration through physical activation method. The effects of varying more production parameters will also be evaluated on specific properties of the activated carbon for solid adsorption refrigeration.

References

[1] Putshak'a, J. D. and Adamu, H. I. (2010). Production and Characterization of Activated Carbon from Leather Waste, Sawdust, and Lignite, Chemsearch J., 1(1): 10 – 15. Publication of Chemical Society of Nigeria, Kano Chapter.

[2] Tadda, M.A., Ahsan, A., Shitu, A., ElSergany, M., Arunkumar, T., Jose, B., Razzaque, M. A. and Nik Daud, N. N. (2016). A review on activated carbon: process, application and prospects, J. Adv. Civil Eng. Pract. and Research, 2(1):7-13.

[3] Shafeeyan, M. S., Wan Daud, W. A., Houshmand, A. and Shamiri, A. (2010). A review on surface modification of activated carbon for carbon dioxide adsorption, J. Analytical and Appl. Pyrolysis, 89: 143–151.

[4] Karthikeyan, S., Sivakumar, P. and Palanisamy, P.N. (2008). Novel activated carbons from agricultural wastes and their characterization. E-Journal of Chem., 5: 409- 426.

[5] Hui, T. S. and Zaini, M. A. A. (2015). Potassium hydroxide activation of activated carbon: a commentary, Carbon Lett., 16:275–280.

[6] Ukanwa, K. S., Patchigolla, K., Sakrabani, R., Anthony E. and Mandavgane, S. (2019). A Review of Chemicals to Produce Activated Carbon from Agricultural Waste Biomass, Sustainability, 2019, 11, 6204.

[7] Sugumaran, P., Priya Susan, V., Ravichandran, P. and Seshadri, S. (2012). Production and Characterization of Activated Carbon from Banana Empty Fruit Bunch and *Delonix regia* Fruit Pod, J. Sustain. Energy & Environ., 3: 125-132.

[8] Zhang, Z., Luo, X., Liu, Y., Zhou, P., Ma, G., Lei, Z. and Lei, L. (2015). A low cost and highly efficient adsorbent (activated carbon) prepared from waste potato residue, J. Taiwan Inst. of Chem. Eng., 49: 206-211.

[9] MartínezMendoza, K. L., BarrazaBurgos, J. M., MarriagaCabrales, N., MachucaMartinez, F., Barajas, M., and Romero, M. (2020). Production and Characterization of Activated Carbon from Coal for Gold Adsorption in Cyanide Solutions, Ingeniería e Investigación, 40(1), 3444.

[10] Leimkuehler, E. P. (2010). Production, Characterization, and Applications of Activated Carbon, Master of Science Thesis presented to the Faculty of the Graduate School University of Missouri, pp. 30-52.

[11] Lua, A. C. and Guo, J. (2001). Microporous oil-palm-shell activated carbon prepared by physical Activation for gas-phase adsorption, Lagmuir, 17: 7112-7117.

[12] Wu, F.C. and Teng, R.L. (2006). Preparation of highly porous carbon from fir wood by KOH etching and CO_2 gasification for adsorption of dyes and phenols from water, J. of Colloid Interface Sci., 294: 21- 30.

[13] Tounsadi, H., Khalidi, A., Farnane, M., Abdennouri, M. and Barka, N. (2016). Experimental design for the optimization of preparation conditions of highly efficient activated carbon from Glebionis coronaria L. and heavy metals removal ability, Process Safety and Environ. Protection, 102: Pages 710-723.

[14] Kosheleva, R. I., Mitropoulos, A. C. and Kyzas, G. Z. (2019). Synthesis of activated carbon from food waste, Environ. Chem. Lett., 17:429–438.

[15] Xia, H.Y. and Peng, J. P. (2007). Preparation of Activated Carbon from Lignin Obtained by Straw Pulping by KOH and K_2CO_3 chemical Activation, Cellulose Chemistry and Tech., 46: 79- 85.

[16] Yahya, M. A., Al-Qodah, Z. and Ngah, C. Z. (2015) Agricultural bio-waste materials as potential sustainable precursors used for activated carbon production: a review, Renew. Sustain. Energy. Rev., 46: 218–235.

[17] Wang, N. and Su, W. (2006). Preparation of activated carbon from coconut shell with steam activation, Carbon, 2: 44- 48.

[18] Pallarés, J., González-Cencerrado, A. and Arauzo, I. (2018). Production and characterization of activated carbon from barley straw by physical activation with carbon dioxide and steam, Biomass Bioenergy, 115:64–73.

[19] Nwabanne, J. T. and Igbokwe P. K. (2011). Preparation of activated carbon from nipa palm not: Influence of preparation conditions, Res. J. of chem. sch., 1(6): 53-58.

[20] Yahya, M. A., Cwingah, C., Hashim, M.A and Al-Qodah, Z. (2015). Preparation of Activated carbon from Desiccated Coconut Residue by Chemical Activation with NAOH, J. of Materials Sci. Research, 5(1): 24.

[21] Park, J. E., Lee, G. B., Hwang, S. Y., Kim, J. H., Hong, B. U., Kim, H. and Kim, S. (2018). The effects of methane storage capacity using upgraded activated carbon by KOH, J. of Appl. Sci., 8: 1596.

[22] Menendez-Diaz A. and Martin-Gullon I. (2006). Types of Carbon Adsorbents and Their Production in Activated Carbon Surfaces in Environmental Remediation, edited by Bandosz T. J. (Academic Press, New York), pp. 1-47.

[23] Efeovbokhan, V. E., Alagbe, E. E., Odika, B., Babalola, R., Oladimeji,, T.E. Abatan, O.G. and Yusuf, E.O. (2019). Preparation and characterization of activated carbon from plantain peel and coconut shell using biological activators, J. Physics: Conference Series, 1378 (2019) 032035, IOP Publishing.

[24] Gopinath, A. and Kadirvelu, K. (2018). Strategies to design modified activated carbon fibers for the decontamination of water and air, Environ. Chem. Lett., 16:1137–1168.

[25] Islam, M. A., Ahmed, M., Khanday, W. et al (2017). Mesoporous activated carbon prepared from NaOH activation of rattan (*Lacosperma secundiflorum*) hydrochar for methylene blue removal, Ecotoxicol. Environ. Saf., 138:279–285.

[26] Koehlert, K. (2017). Activated Carbon: Fundamentals and New Applications, Chemical Engineering, 32 – 40. www.chemengonline.com.

[27] Heidarinejad, Z., Dehghani, M. H., Heidari, M., Javedan, G., Ali, I. and Sillanpää, M. (2020). Methods for preparation and activation of activated carbon: a review, Environ. Chem. Lett., 18: 393–415.

[28] Hu, Z. J. and Li, C. (2008). Study on preparation of active carbon from rice hull steam activation, Biome. Chem. Eng. 41: pp. 21- 24.

[29] Girish, C. R. and Murty, V. R. (2012). Adsorption of Phenol from Wastewater Using Locally Available Adsorbents. Review Paper, J. of Environ. Research and Dev., 6 (3A): 763-772.

[30] Adebayo, G. A. and Aloko, D. F. (2007). Production and characterization of activated carbon from agricultural waste (Rice-husk and Corn-cob), J. of Eng. and Appl. Sci., 2(2): 440-444.

[31] Akpen, G. D., Nwaogazie, I. L. and Leton, T.G. (2011a). Optimum Conditions for the Removal of Color from Wastewater by Mango Seed Shell Based Activated Carbon. Indian J. of Sci. and Technol., 4(8): 890-894.

[32] Kwaghger, A., Kucha,E. I. and Iortyer, H. A (2012b). Experimental Analysis on use of Mango nuts as Adsorbent for solid Adsorption Refrigeration, Int. J. of Scientific and Eng. Research, 13(8): 758-766.

[33] Kwaghger, A., Kucha, E. I. and Iortyer, H. A. (2012a). Optimization of Conditions for the Preparation of Activated Carbon from Mango Kernels Using $CaCl_2$, Int. J. of Env. and Bioenergy, 1(3): 146-161.

[34] Hu, E.J. (1998). A study of thermal decomposition of methanol in solar powered adsorption refrigeration systems. Sol. Energy, 62(5): 325-329.

[35] Kai, E.A.V. and Wang, P.E. (2011). New opportunities for solar adsorption refrigeration, ASHRAE Journal, 53 (9): 14.

[36] Chu, H., Chien, T. W. and Twu, B. W. (2004). The absorption kinetics of NO in $NaClO_2$/NaOH solutions, J. of Hazardous Materials, 84: 241–252.

[37] Cabal, B., Budinova, T., Ania, C. O., Tsyutsarski, B., Panaand, J. B. and Petrova, B. (2009). Adsorption of naphthalene from aqueous solution on activated carbons obtained from bean pods, J. of Hazardous Materials, 161: 1150-1156.

[38] Huang, Y. and Zhao, G. (2016). Preparation and characterization of activated carbon fibers from liquefied wood by KOH activation, Holzforschung, 70:195–202.

[39] Saha, B. B., Koyama, S., Kashiwagi, T., Akisawa, A., Ng, K.C and Chua, H.T. (2003). Waste heat driven dual-mode, multi-stage, multi-bed regenerative adsorption system, Int. J. of Refrigerant, 26: 749–757.

[40] Saha, B. B., Akisawa, A. and Kashiwagi, T. (2001). Solar/waste heat driven two-stage adsorption chiller, J. of Renew. Energy, 23:9.3-101.

[41] Deng, H., Yang, G., Li, H., Jiping, T. and Jiangyun.T. (2010). Preparation of activated carbons from cotton stalk by microwave assisted KOH and K_2CO_3 activation, Chem. Eng. J., 163: 373- 381.

[42] Hamamoto, Y., Alam, K. C. A., Saha, B. B., Koyama, S., Akisawa, A., Kashiwagi, T. (2006). Study on adsorption refrigeration cycle utilizing activated carbon. Adsorption characteristics, Int. J. of Refrigeration, 29: 305-314.

[43] Critoph, R. E. and Metcalf, S. J. (2004). Specific cooling power intensification limits ammonia- carbon adsorption refrigeration systems, Appl. Therm. Eng., 24(5-6): 661- 678.

[44] Aristov, Y. I. (2007). New family of solid sorbents for adsorptive cooling: Material scientist approach, J. of Eng. Thermophysics, 16:63-72.

[45] Al-Mousawi, F. N., Al-Dadah, R. and Mahmoud, S. (2016). Low grade heat driven adsorption system for cooling and power generation using advanced adsorbent materials, Energy Conv. and Mgt., 126:373-384.

[46] Zheng, A. and Gu, J. (2006). Advanced solar- powered rotary solid adsorption refrigerator with high performance Renewable Energy Resources and Greener Future. 6th International Conference for Enhanced Building Operation. Shenzhen, China. 3: 721- 739.

[47] Ullah, K. R., Saidur, R., Ping, H.W., Akikur, R.K. and Shuvo, N.H. (2013). A review of solar thermal refrigeration and cooling methods, Renew. and Sustain. Energy Reviews, 24:499-513.

[48] Wang, L.W., Wang, R.Z. and Oliveira, R.G. (2009). A review on adsorption working pairs for refrigeration. Renew. & Sustainable Energy Reviews, 13(3): 518- 534.

[49] Mande S., Ghosh P. and Kishore V. V. N. (1996). Development of an Advanced Solar-hybrid Adsorption Cooling System for Decentralised Storage of Agricultural Products in India; DLR-TERI Joint project report; submitted to The Commission of the European Communities, pp. 2-3.

[50] Abasi, C. Y., Abia, A. A. and Igwe, J. C. (2011). Adsorption of Iron (III), Lead (II) and Cadmium (II) ions by unmodified Raphia palm (Raphia Hookeri) fruit endocarp, Environ. Research J., 5(3): 104-113.

[51] Akpen, G. D., Okparaku, L. A. and Odoh, F. O. (2011b). Removal Of Colour From Wastewater By Raffia Palm Seed Activated Carbon, J. of Emerging Trends in Eng. and Appl. Sci., 8(1): 25-29.

[52] Edem, D.O., Ekaande, O.U., Ifon, T. (1984). Chemical evaluation of the nutritive value of the Raffia palm fruit (Raphia hookeri), Food Chemistry, 15: 9–17.

[53] Elizalde-Gonzalez, M. P. and Hernandez-Montoya, V. (2007). Characterization of raphia pit as raw material in the preparation of activated carbons for wastewater treatment, Biochem Eng. J., 36: 230- 238.

[54] Kwaghger, A., Edeoja, A. and Tile, J. (2015). Comparative Study of Isotherms of Activated Carbons Produced from Mango Kernels and Commercial Activated Carbons (ISO 9001:2000), J. of Energy Techs. and Policy, 5(2).

[55] Abdulrazak, S., Hussaini, K. and Sani, H. (2016). Evaluation of removal efficiency of heavy metals by low-cost activated carbon prepared from African palm fruit, Applied Water Science. 10.1007/s13201-016-0460-x. Springer.

[56] Pathania, D., Sharma, S. and Singh, P. (2017). Removal of methylene blue by adsorption onto activated carbon developed from Ficus carica bast, Arabian Journal of Chemistry, 10(1): S1445-S1451.

[57] Tan, I. A. W., Hameed, B. H. and Ahmad, A. L. (2007). Equilibrium and kinetic studies on basic dye adsorption by oil palm fibre activated carbon, Chemical engineering journal, 127(1-3): 111-119.

[58] Sahu, J. N., Achrya, J. and Meikap, B. C. (2010). Optimization of production conditions for activated carbons from Tamarind wood by zinc chloride using response surface methodology. Bio Res. Tech., 101.

[59] Walhof, L.K. (1998). Procedure to produce activated carbon from bio solids. Illinois Institute of Technology Chicago. Master's thesis. pp19.

[60] Ahmed, M. J. (2016). DOE++ 9 Quick Start Guide. Response Surface Method for Optimization, Environ. and Chem. Eng., 4(1): 89–99.

[61] Tie, M., Liang C., Shan-zhi X., and Xin-ming Y., (2015). Activated Carbon from the Chinese Herbal Medicine waste by H_3PO_4 activation, J. of Nanomaterials, 20: 110-115.

[62] Liu, B., Gu, J. and Zhou, J. (2016). High surface area rice husk-based activated carbon prepared by chemical activation with $ZnCl_2$–$CuCl_2$ composite activator, Environ. Prog. Sustain. Energy, 35:133–140.

[63] Li, J., Ng, D. H., Song, P. et al (2015). Preparation and characterization of high-surface-area activated carbon fibers from silkworm cocoon waste for Congo red adsorption, Biomass Bioenergy, 75:189–200.

[64] Li, S.Q., Yao, S.E., Wen, Y. Chi and Yan. J.H. (2005). Properties of pyrolytic chars and activated carbons derived from pilot- scale pyrolysis of used tyre, J. Air Waste Manag. Assoc., 55(9): 1315- 1341.

[65] Wang, R. Z., Jia, J.P., Teng, Y., Zhu, Y. H. and Wu, J. Y. (1997). Study on a new solid adsorption refrigeration pair, active carbon fiber–methanol, ASME J. of Solar Energy Eng., 119: 214- 218.

[66] Kays, W.M. and Crawford, M.E. (1993). Convection heat and Mass Transfer. 3rd Edition, McGraw-Hill, New York, pp.88-102.

[67] Osarenmwinda, J.O and Imoebe, S. (2008). Improved saw dust briquette: An Alternative Source of Fuel, Conference Proceedings, ICERD, University of Benin. pp. 98.

[68] Lu. Z. S., Wang, R. Z. Wang L. W. and Chen, C. J. (2006). Performance analysis of an adsorption refrigerator using activated carbon in a compound adsorbent, Carbon, 44(4): 747- 752.

[69] Satish, G.N. K. (2015). Multiple response analysis using SPSS. YouTube. My Easy Statistics.

[70] John, W. (2003) Applied Statistic and Probability for Engineers. Montgomery and Runger. Microsoft power point presentation on design of experiment with several factors. 14. Pp, 5-121.

[71] Yorgun, S. and Yıldız, D. (2015). Preparation and characterization of activated carbons from Paulownia wood by chemical activation with H_3PO_4, J Taiwan Inst. Chem. Eng., 53:122–131.

[72] Shamsuddin, M., Yusoff, N. and Sulaiman, M. (2016). Synthesis and characterization of activated carbon produced from kenaf core fiber using H_3PO_4 activation, Procedia Chem., 19:558–565.

[73] Yakout, S.M. and Sharaf El-Deen, G. (2012): Characterization of activated carbon prepared by phosphoric acid activation of olive stones, Arabian J. of Chem., 1016.

[74] Demiral, İ. and Şamdan, C. A. (2016). Preparation and characterisation of activated carbon from pumpkin seed shell using H_3PO_4. Anadolu Univ. J. Sci. Technol. & Appl. Sci. Eng., 17:125–138.

[75] Hesas, R. H., Arami-Niya, A., Wan Daud, W. A. and Sahu, J. N. (2013). Preparation and Characterization of Activated Carbon from Apple Waste by Microwave-Assisted Phosphoric Acid Activation: Application in Methylene Blue Adsorption, BioResources, 8(2): 2950-2966.

[76] Xu, J., Chen, L., Qu, H., Jiao, Y., Xie, J. and Xing, G. (2014). Preparation and characterization of activated carbon from reedy grass leaves by chemical activation with H_3PO_4, Appl. Surface Sci., 320: 674-680.

[77] Laine, J., Calafat, A. and Labady, M. (1989). Preparation and characterization of activated carbons from coconut shell impregnated with phosphoric acid, Carbon, 27: 191- 195.

[78] Shalna, T. and Yogamoorthi, A. (2015). Preparation and Characterization of Activated Carbon from Used Tea Dust In Comparison with Commercial Activated Carbon, Int. J. of Recent Scientific Research, 6(2): 2750-2755.

[79] Wang, X., Zimmermann, W., Ng, K., Chakraboty, A. and Keller J. (2004). Investigation on the isotherm of silica gel-water systems, J. of Thermal Analysis and Calorimetry, 76: 659-669.

[80] Boubakri, A., Guilleminot J.J., and Meunier. F. (2000). Adsorptive solar powered ice maker: experiments and model, Sol. Energy, 69: 249-312.